A New drying Preparation of PZT Powders Chemically Derived by Sol-gel process

Tien-I Chang*[1], Jow-Lay Huang*[1] and Jen-Fu Lin[1], Bing-Huei Chen[2] and Long Wu[2,3]

[1]Department of Material Science and Engineering, National Cheng-Kung University, No.1 University Road, Tainan 701,Taiwan, ROC

[2] Department of Electrical Engineering, National Cheng-Kung University, No.1 University Road, Tainan 701, Taiwan, ROC

[3]f-tech Corporation, No.16 Nan-Ke 9th Road, Science-based Ind. Park, Tainan 741, Taiwan, ROC

Postal address: No.29, Dongfong Rd., North District, Tainan City 704, Taiwan (R.O.C.)
***Corresponding author, takashi@cubic.mat.ncku.edu.tw, JLH888@mail.ncku.edu.tw,**

Fax: +886-6-2763586 or +886-6-2766464

Abstract

Pure pervoskite phase $Pb_{1.15}(Zr_{0.53}Ti_{0.47})O_3$(PZT) powders were prepared by a chelating acetate sol-gel process. Powders obtained from two different heating temperature, namely as-dried H.T powders(300^{o}C/30mins) and as-dried L.T powders(150^{o}C /10hrs) were

analyzed. Both of those PZT powders were investigated by Fourier transform infrared spectroscopy(FT-IR), differential thermal analysis/ thermal gravimetric analysis(DTA/TGA) and Transmission Electron Microscope(TEM). The combined results indicate that as-dried H.T powders contained a higher mole fraction of acetate groups and that polycondensation was slower, resulting in a smaller particle size. It is a better and shorter heating period, low-budget, and more energy-economized procedure compared with the conventional heating temperature, such as as-dried L.T powders.

Keywords:

PZT, ferroelectrics, sol-gel, the morphotropic phase boundary

1. Introduction:

Lead zirconate titanate(PZT) is an important ferroelectrics material possessing good piezoelectric and pyroelectric properties with important technological applications1-3). It has been used widely since the 1950s in electronic components and devices such as ultrasonic-audio tone transducers, electrical resonators, wave filters, sensors and actuators. It is known that, PZT has a non-centrosymmetric ABO_3 perovskite type structure. The piezoelectric activity in the solid solution $PbZrO_3$-$PbTiO_3$ system is optimum for compositions near the morphotropic phase boundary(MPB). The MPB is an almost-

temperature-independent phase boundary that separates two ferroelectrics phases: a tetragonal phase(F_T,P4mm) and a rhombohedral phase(F_R,R3c).

A coexistance of phases occurs due to a compositional fluctuation(different chemistry potential caused by non-homogeneity) of Zr^{+4} and Ti^{+4} ions in the PZT structure. Compositions near the MPB may have both of those two phases coexisting to give a total of fourteen possible polarization directions(six tetragonal□001□ and eight rhombohedral□111□---in reference to the cubic prototype cell axes). The large number of polarization directions enables optimized crystallographic orientations to be established from grain to grain in the polarization process and, in turn, results in anormalously high pizoelectric properties. In lead zirconate titanate preparation, the control of some parameters is important to achieve the desired material properties. These parameters include the absence of intermediate crystalline phase like pyrochlore phase, a defined and a fixed stoichiometry, as well as a homogeneous lead distribution in the microstructure.

For the solid-state reaction method, due to intermediate reactions that lead to formation of $PbTiO_3$(PT) and $PbZrO_3$(PZ), the PZT formed by this method is heterogeneous in composition. However, PZT powder synthesized by chemical methods such as sol-gel process has resulted in powder with low compositional fluctuation, narrow MPB, and reactive powders 4-6).

In recent years, there has been a considerable interest in using the sol-gel process to prepare ceramics and glasses from metal alkoxides 7-9). Such as the sol-gel process can be used to produce high purity, ultra-fine particles and large-area thin films at relatively low temperatures. The properties of the resulting PZT powders depend on the choice of metal alkoxides and solvents, solution concentration, Zr to Ti ratio as well as the rate of drying.

Common precursors for the sol-gel preparation of ferroelectrics are metal alkoxides. Metal alkooxides are soluble in common solvents and can be polymerized though hydrolysis and condensation. In particular, lead acetate trihydrate [$Pb(CH_3CO_2)_2.3H_2O$] is chosen as a precursor for lead because lead alkoxides are unstable and are not soluble in common solvents.

In practice, the alkoxide solution is stabilized against uncontrolled hydrolysis by chemical modification, or by the introduction of chelating agents to produce the number of active functional groups and thereby lower its reactivity with water. Examples of chemical modifiers are 2-methoxyethanol (2-MOE) or acetic acid.

In this study, the sol-gel process prepared PZT powder by using zirconium n-propoxide, titanium iso-propoxide and lead acetate trihydrate as precursor. The solution obtain from sol-gel process was identified by NMR, and the bonding conditions was analyzed by FT-IR. The structural variation of $Pb_{1.15}(Zr_{0.53}Ti_{0.47})O_3$ powders with different calcined temperature was studied by differential thermal analysis(DTA), thermo-gravimetric analysis(TGA). Compared with conventional powder-produced process(i.e. L.T powders), this studies chose higher temperature and shorter procedure period(i.e. H.T powders) as a new powder-produced condition to compare the difference of the particles size distribution and phase transformation temperatures.

2. Experimental procedures:

Fig.1 shows the experimental procedure of this study. Lead acetate trihydrate was first dissolved in propyl alcohol(ACROS Organics density 0.8 g/cm^3, purity 99%) with the amount of 10g to 1ml at 80^oC in a three-neck reaction glass container. The solution was

then heated to 120^{o}C and maintained for 2hr to remove the residual water, and naturally cooled to 80^{o}C. A stoichiometric amount of zirconium n-propoxide(23~28 free alcohol, density 1.05g/cm^{3}, purity 75%)and acetic acid(TEDIA, density 1.059 g/cm^{3})were added to the lead acetate solution and refluxed at 120^{o}C for 1hr to form PZ solution. The ratio of lead acetate to acetic acid to propyl alcohol is 10□5□1. After that, titanium iso-propoxide(density 0.7550g/cm^{3}, purity 98%)was added to the PZ solution and further refluxed at 120^{o}C for 2hr, to form the PZT solution. NMR analysis of as-prepared PZT solution was performed by using a C^{13}NMR spectrum in deuterated benzene(C_6D_6).

PZT stock solution was used to produce high-temperature-prepared powder; namely H.T powders(dried at 300^{o}C for 30min)and low-temperature-prepared powders; namely L.T powders (dried at 150^{o}C for 10hr). FT-IR spectra of as-dried PZT powders were obtained by using a JASCO FT-IR-460 plus with a wave number ranging from the 400 to 4000 cm^{-1}.

After that, H.T. and L.T. powders were characterized with a laser particle size distribution analyzer(Malvern Instruments) and Transmission Electron Microscope(HITACHI FE-2000 Field Emission Transmission Electron Microscope). DTA(differential thermal analyzer)/ TGA(thermo-gravimetric analyzer)was carried out on using Al_2O_3 as the reference.

3. Results and Discussion:

3.1 C^{13} NMR analysis

Fig.2 shows the C^{13} NMR spectrum of the as-prepared PZT solution in deuterated benzene(C_6D_6). The resonance peak at 10.39, 25.94, 64.01, and 178.04 ppm can be attributed to the carbon bonds of both the propyl alcohol and acetic acid, and designated by

"a" to "d". According to the NMR index, the peaks at 128 ppm(127.77, 128.01, 128.25 ppm) were due to the deuterated benzene(C_6D_6). The peak at 172.14 ppm(designated as "e") was interesting, may be attributed to the formation of a small amount of ester, a by-product during the polymeric reaction.

The origin of this ester is apparent considering the reactions involved in the preparation of the lead precursor. It has been determined that in the synthesis route followed, one alkoxy group replaces one of the acetate groups:

$Pb(OAc)_2 + ROH \rightarrow Pb(OAc)(OR) + AcOH$ (1)

Where R = $CH_3CH_2CH_2$- , and Ac = CH_3CO-

The acid thus produced AcOH reacts with the solvent propyl alcohol to form an ester:

$AcOH + ROH \rightarrow AcOR + H_2O$ (2)

It releases a certain amount of free water into the system. If this free water is not removed by distillation, some preliminary hydrolysis and condensation reactions can occur on combining with the Zr/Ti precursor solution leading to a degree of in-homogeneity in the solution 17). As mentioned above, after lead acetate trihydrate dissolved in propyl alcohol at 80^{o}C, it is necessary to dehydrate the lead acetic solution.

Acetic acid reacts with zirconium propoxide and titanium isopropoxide to form titanium isopropoxide monoacetate and zirconium propoxide diacetate, respectively 11).The alcohol formed in the reaction also reacts with acetic acid to produce esters. The acetate group likely act as bridging ligands bonded to two metal ions to form structures such as bridging structure of titanium alkoxide acetate 12).

3.2 DTA/TGA analysis

DTA/TGA was performed on the H.T and L.T powders at a heating rate of 10^{o}C /min.

The DTA curve shows an endothermic peak at 100°C for H.T powders(Fig.3a) and 89°C for L.T powders(Fig.3b), primarily due to the removal of alcohol and water absorbed in the PZT solution. The exothermic peak at 320°C(H.T powders) and 319°C(L.T powders) together with the corresponding larger weight loss, can be attributed to the decomposition of the residual lead acetate14). The two exothermic peaks at 515°C and 580°C for H.T powders and 505°C and 553°C for L.T powders are due to the use of complex alkoxide precursors.

K. D. Budd et al. 13) did some DTA/TGA work on a series of single alkoxide, and found a single and sharp exothermic peak. On the other hand, their studies on the complex alkoxides showed broad and wide-range distributed exothermic peaks, and reported that the number of peaks and peak shapes were affected by composition of precursors and the amount of water.

As to the broadened exothermic peaks at 515°C for H.T and 505°C for L.T powders, it should be attributed to the reaction of bonds break in the PZT polymer or the formation of inorganic ceramic phase. And the exothermic peaks at 580°C for H.T and 553°C for L.T powders should be correlated to the phase transition of PZT, because no weight loss could be found in TG curve. As a result, crystallization of PZT powders take place at the range of 500°C to 515°C, and perovskite structure is established above 580°C for H.T powders and above 550°C for L.T powders. Taking these observations into consideration, the first exothermic peak is considered to be predominantly caused by the formation of the meta-stable pyrochlore phase and the second one by the perovskite phase formation, both accompanied by the residual combustion of the organics. The observed crystallization of pyroclore phase at temperatures between 450°C and 500°C its transformation to the

perovskite phase in the temperature range from 500°C to 600°C, are quite typical for many sol-gel-derived PZT powders13,23-25) . The individual temperatures where the DTA peaks appear in the different samples depend on the precursor chemistry. Above 600°C the TGA curve shows no significant decrease in weight and this is the staring temperature, which was chosen as the calcined temperature of the powders.

The total weight loss observed in the TGA analysis shows that the as-dried H.T powder contained 80wt% PZT, and the as-dried L.T powder contained 83wt% PZT. Therefore, the as-dried H.T powder contained more organic species. The biggest portion of organic species should be acetate group, because the heating period(30min) is shorter for as-dried H.T powder than this(10hr) for as-dried L.T powder. W. D. Yang 14) stated that the higher amount of acetate groups in the gel structure is responsible for an increased distance between the cations(Pb^{2+},Zr^{4+},Ti^{4+} etc.) in the structure. It results in an inhibition of the formation of PZT for H.T powder. This necessitates a higher reaction temperature for the formation of PZT.

Also, it was observed that for H.T powders those peaks correspond to relative temperatures all higher than L.T powders. It is due to incompletely removal organics solvent during as-dried H.T powders were prepared. But for L.T powders, it has longer time to produce fewer amounts of organic as-dried powders. It also can be confirmed later from FT-IR analysis as discussed in 3-3.

3.3 FT-IR analysis

The FT-IR technique was employed to monitor the chemistry of the aqueous acetate-based process. Fig. 4(a) shows the FT-IR results of the PZT stock solution. Since titanium isopropoxide monoacetate was formed from titanium iso-propoxide, acetic acid, and water.

The PZT stock solution should contain lead acetate, titanium isopropoxide monoacetate and zirconium propoxide diacetate, the excess acetic acid and water, a trace amount of un-reacted titanium isopropoxide, and also the product of isopropanol. Notice that titanium isopropoxide has not been completely consumed; it should otherwise exhibit sharp bands around 2960, 2930, and 1465, 1375cm^{-1}, respectively, corresponding to the stretching and bending vibrations of the aliphatic CH_2 and CH_3 groups. Moreover, a series of three bands should also apper on the low energy side of the spectrum, below 1125cm^{-1} corresponding to the Ti-O-C vibrations of isopropoxy groups directly bonded to titanium 19) and a band at 1144cm^{-1} attributed to the Zr-O-C stretching vibration of the propoxy groups of zirconium propoxide21).

The spectral assignment can be made as follows :(1) The broad band extending from 3600 to 2800cm^{-1} can be assigned to the stretching modes of ν_{OH} and ν_{CH} of isopropanol, water, acetic acid, and acetate organic moieties. (2) Two bands around 1720cm^{-1} and 1255cm^{-1} could be attributed to the ν(coo-) vibrations of an acetate ligand but the large frequency separation($\Delta\nu$= 465 cm^{-1}) between the ν_{sym}(1255 cm^{-1}) and theν_{asym}(1720cm^{-1}) suggests an unidentate acetate ligand. (3) In the low energy spectral region, the bands at 1017cm^{-1} are the C-H rocking mode, the band at 960cm^{-1} can be assigned to the C-O vibration of the propanol22) whereas the 944cm^{-1} peak belongs to the C-C stretching vibration of the organic functionalities.

The FT-IR spectroscopy was also used to monitor the steps of the powder formation with different heat-treatment temperature. Fig.4 (b) and (c) show FT-IR spectra of H.T and L.T powders before calcination, respectively. It is found that both of them had the same bonding condition and similar characters to the spectra obtained by Yang 14). The broad

bands at approximately 3400cm^{-1} are attributed to OH stretching vibrations due to the H_2O and hydroxyls present in the systems. There were two absorption bands in the vicinities of 1411 and 1551cm^{-1} for H.T powder (Fig.4 (b)) and 1409 and 1557cm^{-1} for L.T powder (Fig.4 (c)). These peaks were attributed to the symmetric(ν_{sym} (coo-)) and asymmetric vibrations(ν_{asym} (coo-)) of the acetate group, respectively. The free acetate ion has 15 infrared active fundamentals of which the asymmetric and symmetric stretching modes of the coo- group have been selected for structural studies. For the free acetate ion, the ν_{asym} (coo-) andν_{sym} (coo-) are approximately 1560cm^{-1} and 1416cm^{-1}, respectively, giving Δ(free) □144 cm^{-1} ($\Delta\nu$, $\Delta\nu=\Delta(\nu_{asym} - \nu_{sym})$) 18). When the difference between those two absorption peaksΔvis smaller than 80cm^{-1}, acetate is typically a chelating bidentate ligand. When Δvis larger than 160cm^{-1}, the acetate group is typically a bridging bidentate ligand[15].

The value of $\Delta\nu$ was 140cm^{-1} for H.T powder (Fig.4 (b)), and 148cm^{-1} for L.T powder (Fig.4 (c)). The difference $\Delta\nu$ of L.T powder was larger than that of the H.T powder, meaning that the L.T powder contained more bridging bidentate ligands result in larger particles of the L.T final powder and the H.T powder contained more chelating bidentate ligand lead to a smaller particle size. This is in good agreement with the particle size distributions and TEM observations of as-dried H.T and L.T powders as discussed in 3.4.

3.4 Distribution of particles size for as-dried H.T and L.T powders

The H.T powders and L.T powders were characterized with a laser particle size distribution analyzer. Comparing the particle size distribution of the two different heating conditions, the L.T powders(Fig. 5 (b)), in which the powders contained fewer acetate group as shown in the DTA/TG results of Fig. 3 (b), was found to be less homogeneous(one

is 491.5nm and the other is 1083.7nm). It also had larger aggregate particle sizes compared with as-dried H.T powders(421.2nm)(Fig. 5 (a)).

Livage et al. 20) indicated that the acetate group inhibits the polycondensation process and if chelating acetate groups are present, the structure around the Ti-ions remains intact which was proved in 3-3 FT-IR section, resulting in an inhibition of the condensation process and prolonging the time of gelation. Since the rate of hydrolysis and polycondensation control the aggregate particle size of the precursor sol, a slower rate of polycondensation should lead to a more monodispersed gel with a smaller aggregate particle size. Indeed the H.T powders, which contain a larger portion of organic species, exhibited inhibited powder formation compared with the L.T powders. The H.T powders were, therefore, more homogeneous, contained fewer aggregates and a smaller aggregate particle size.

3.5 TEM analysis of the as-dried powders

The H.T and L.T powders were analyzed by TEM(Fig. 6). Electron diffraction patterns for the H.T powders and L.T powders show the amorphous phase due to un-crystallized. TEM analysis enables the primary particle size of the powders to be determined, as opposed to the particle size distribution given by laser diffraction(Fig. 5). The primary particles of the H.T powders were approximately 300-400nm in diameter(Fig. 6(a)), compared to the L.T powders which were about 400nm or larger in diameter(Fig. 6(b)). For the H.T powders, the smaller particles size could decrease sintering temperatures. Also, the results are in a good agreement with the particle size distribution determined by the laser diffraction.

4. Conclusions:

1. The DTA curve shows an endothermic peak at 100^{o}C for H.T powders and 89^{o}C for L.T powders, primarily due to the removal of alcohol and water absorbed in the PZT solution. The exothermic peak at 325^{o}C (H.T powders) and 319^{o}C (L.T powders) together with the corresponding weight loss, can be attributed to the decomposition of the residual lead acetate and the formation of carbonate. The two exothermic peaks at 515^{o}C and 580^{o}C for H.T powders and 505^{o}C and 550^{o}C for L.T powders are due to the use of complex alkoxide precursors. Above 600^{o}C the TGA curve shows no significant decrease in weight and this is the staring temperature, which was chosen as the calcined temperature of the powders.

2. The FT-IR spectroscopy results show the comparison of H.T powders and L.T powders. It was found that both of them had the same bonding condition and similar to the previous studies. The value of $\Delta\nu$ was 140cm^{-1} for the H.T powder, and 148cm^{-1} for the L.T powder. The difference $\Delta\nu$ of the L.T powder was larger than that of the H.T powder, meaning that the L.T powder contained more bridging bidentate ligands result in larger particles of the L.T final powder and the H.T powder contained more chelating bidentate ligand lead to a smaller particle size.

3. Comparing the particle size distribution of the two different heating condition as-dried powders, the L.T powders, in which the powders contained fewer acetate group as shown in the DTA/TG results, was found to be less homogeneous(one is 491.5nm and the other is 1083.7nm). It also had larger aggregate particle sizes compared with as-dried H.T powders (421.2nm).This new powders-produced procedure will be a better heating condition for further studies.

5. References:

1) Kanai, H., Furukawa, O., Abe, H. and Yamashita, Y.:J. Am. Ceram. Soc. 77 [10] (1994) 2620-2624.

2) Benguigui, L.: Solid State Communication 19 (1986) 979-981.

3) Yamamoto, T.: Ceram. Bull 71 [6] (1992) 978-985.

4) M. A. Zaghete, C. O. Paiva-Santos, J. A. Varela, E. Longo. and Y. P. Mascarenhas: J. Am. Ceram. Soc. 75 [8] (1992) 2089-2093.

5) G. Toimandl, A. Stiegelschmitt, and R. Bohner, Lower the sintering temperature of PZT ceramic by sol gel processing. In Science of Ceramic Chemical Processing Part 1, Sol-Gel Science, ed. L. L. Hench and D. R. Ultrich, Wiley, New York, 1986, pp. 56-.

6) K. Kakegawa, K. aria, Y. Sasaki. and T. Tomizawa: J. Am. Ceram. Soc. 71 [1] (1988) C49-C52.

7) M. Lourdes Calzada, Rafael Sirera, Francisco Carmona, and Basilio Jimenez: J. Am. Ceram. Soc. 78 [7] (1995) 1802-1808.

8) Susan Trolier-McKinstry, Jiayu Chen, Kuppuswami Vedam and Robert E. Newnham: J. Am. Ceram. Soc., 78 [7] (1995) 1907-1913.

9) Yong-Il Park, Masayuki Nagai, Masaru Miyayama and Tetsuichi Kudo: J. of Mat. Sci. 36 (2001) 1995-2000.

11) Yi, G. Ph. D Thesis-Queen's University (1993) (unpublished)

12) Sanchez, C., Toledano, P. and Ribot, F., Molecular structure of metal oxide precursors.

in Better Ceramics through Chemistry Volume 4 San Francisco□Material Research Society, ed. B. J. J. Zelinski, D. E. Clark & D. R. Ulrich, 1990, pp. 47-59.

13) K. D. Budd, S. K. Dey and D. A. Payne: Br. Ceram. Proc. 36 (1985) 107-121.

14) W. D. Yang: Ceram. Inter. 27 (2001) 373-384.

15) C. Sancher, J. Livage, M. Henry and F. Babonneau: J. Non-Cryst. Solids 100 (1988) 65-76.

16) E. R. Leite, M. C., L. A. Perazoli, R. S. Nasar and E. L .: J. Am. Ceram. Soc., 79 [6] (1996) 1563-1568.

17),Factors affecting the sol-gel processing of PZT thin layers. Ferroelectric films,413-439.

18) K. Nakamoto, Infrared and Raman Spectra of Inorganic and Coordination compounds, third edition, John Wiley and Sons, New York, 1978.

19) H. Kriegsmann. K. Licht, and Z. Elek., 62, 1163 (1958).

20) J. Livage, C. Canchez, M. Henry and S. Doeuff.: Solid State Chem., 32/33 (1989) 633-638.

21) D. C. Bradley, R. C. Mehrotra and D. P. Gaur, Metal Alkoxides, Academic Press, New York, 1978.

22) C. J. Pouchert, The Aldrich Library of Infrared Spectra, second edition, Aldrich Company, Milwaukee, WI, 1975.

23) H. Hirashima, E. Onishi and M. Nakawaga: J. Non-Cryst. Solids, 121 (1990) 404-.

24) C. T. Lin, B. W. Scanlan, J. D. Mcneill, J. S. Webb and L. Li: J. Mater. Res. **7** [9] (1992) 2546-.

25) T. Fukui, C. Sakurai and M. Okuyama: J. Mater. Res. **7** [4] (1992) 791-.

6. Figure Captions:

Fig.1 Flow-chart for preparation of (a) PZT(53/47) stock solution (b) H.T and L.T powders

Fig.2 C^{13} NMR spectrum of the as-prepared PZT(53/47) solution and peaks relative to the bondings.

Fig.3 DTA/TG results of (a) H.T, and (b) L.T PZT (53/47) powders

Fig.4 FT-IR spectrums of (a) a new made PZT solution(b)H.T powder, and (c) L.T powder before calcinations

Fig. 5 The particle size distributions of (a) H.T and (b) L.T powders

Fig.6 Bright field TEM micrographs and corresponding electron diffraction patterns for (a) H.T powders and (b) L.T powders

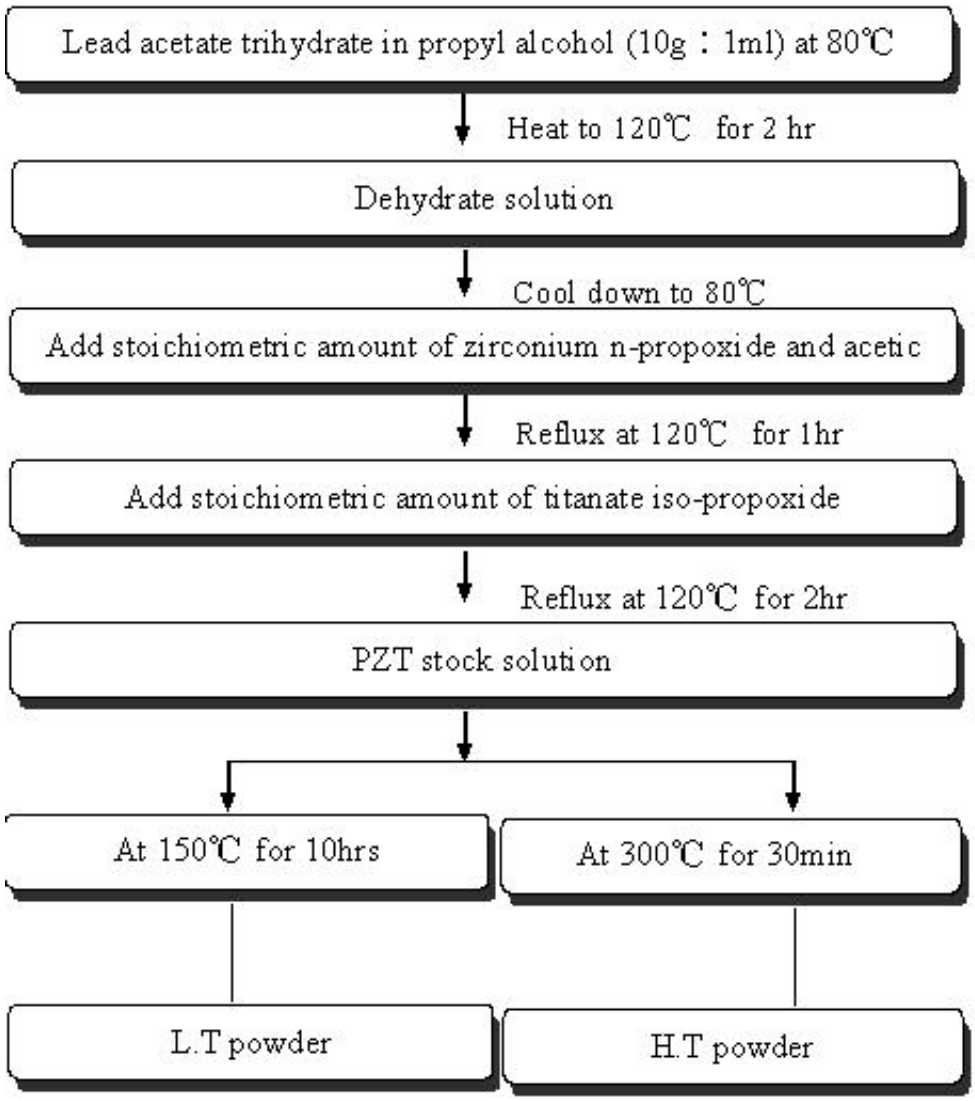

Fig.1 Flow-chart for preparation of PZT (53/47) stock solution, H.T and L.T powders

(a)

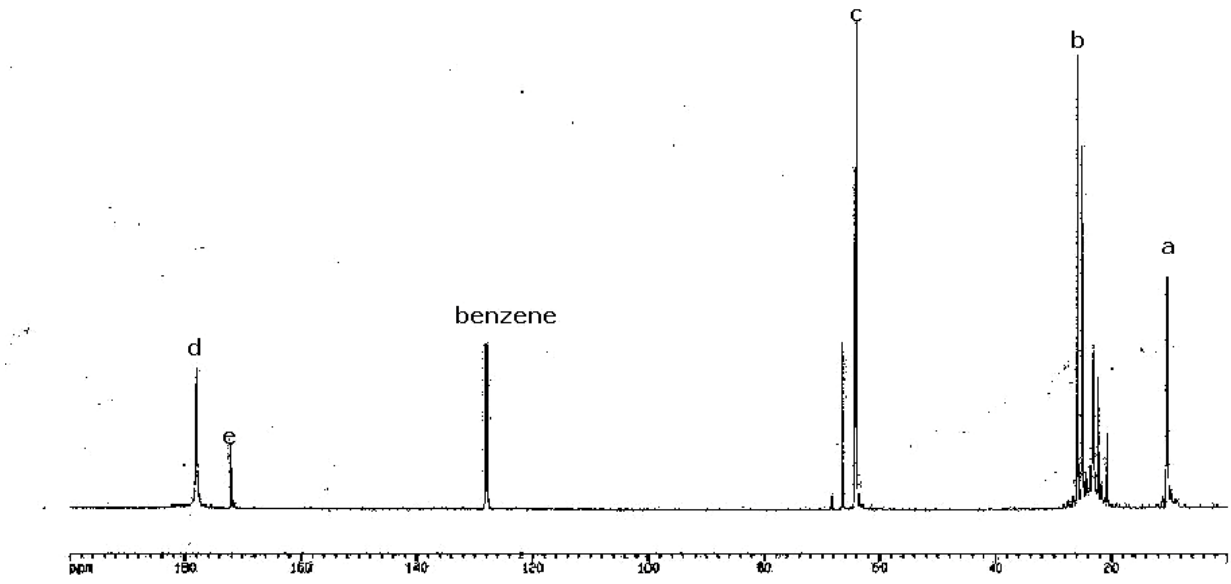

Fig.2 C^{13} NMR spectrum of (a) the as-prepared PZT(53/47) solution and(b) peaks relative to the bondings.

(b)

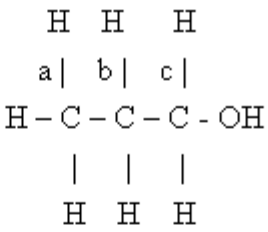

propyl alcohol

a =10.39ppm

b = 25.94ppm

c = 64.01ppm

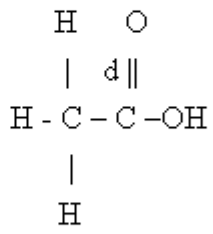

acetic acid

d = 178.04ppm

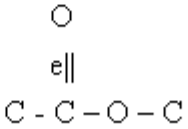

ester

e = 172.14ppm

(a)

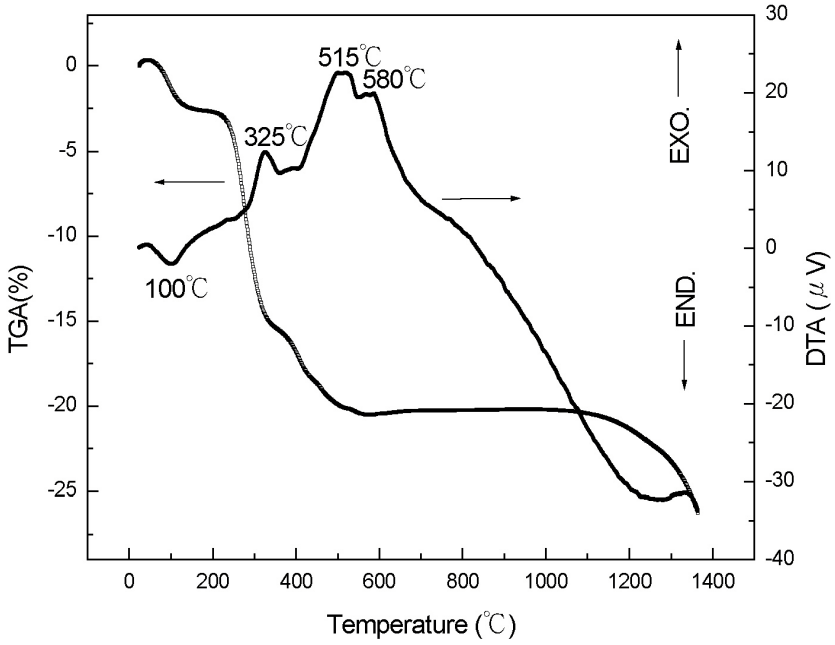

Fig.3 DTA/TG results of (a) H.T, and (b) L.T PZT (53/47) powders

(b)

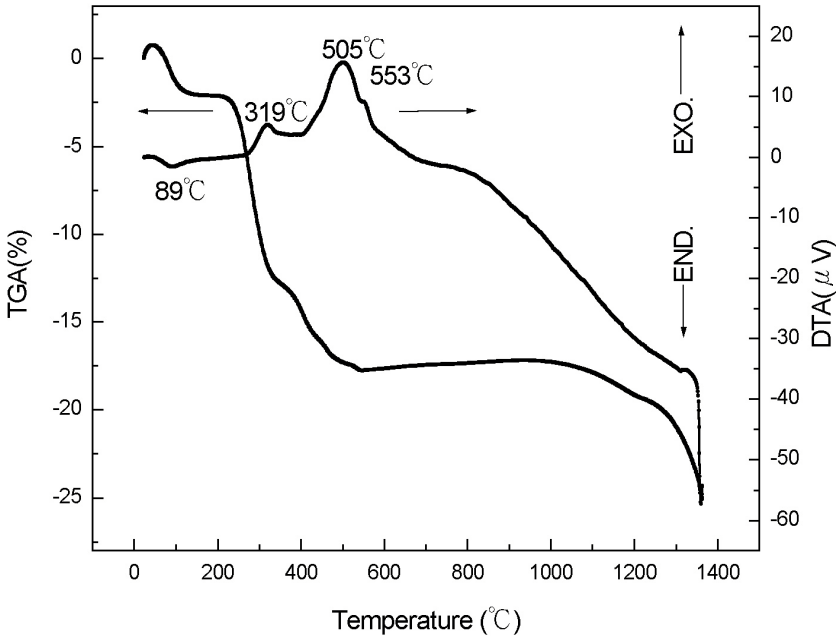
505℃
553℃
319℃
89℃
EXO.
END.
TGA(%)
DTA(μV)
Temperature (℃)
0
-5
-10
-15
-20
-25
20
10
0
-10
-20
-30
-40
-50
-60
0
200
400
600
800
1000
1200
1400

(a)

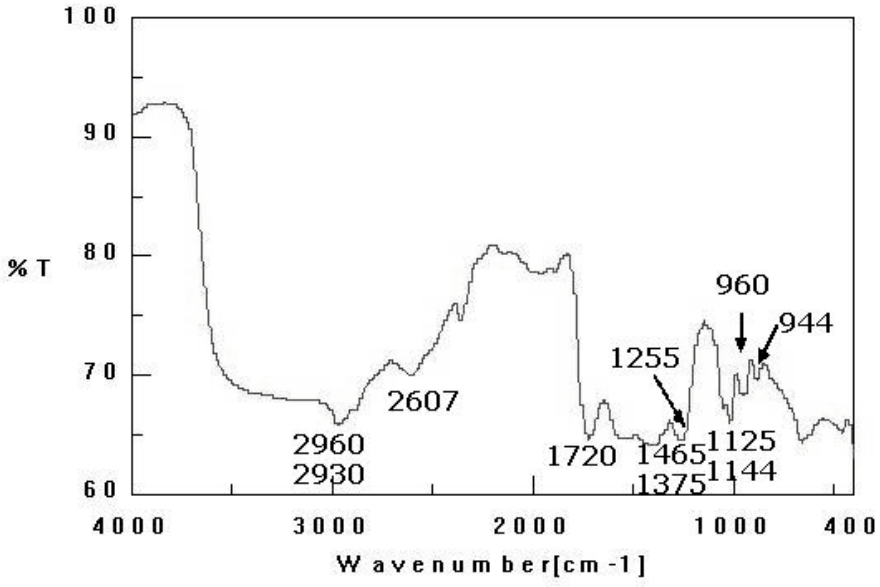

Fig.4 FT-IR spectrums of (a) a new made PZT solution(b)H.T powder, and (c) L.T powder before calcinations

(b)

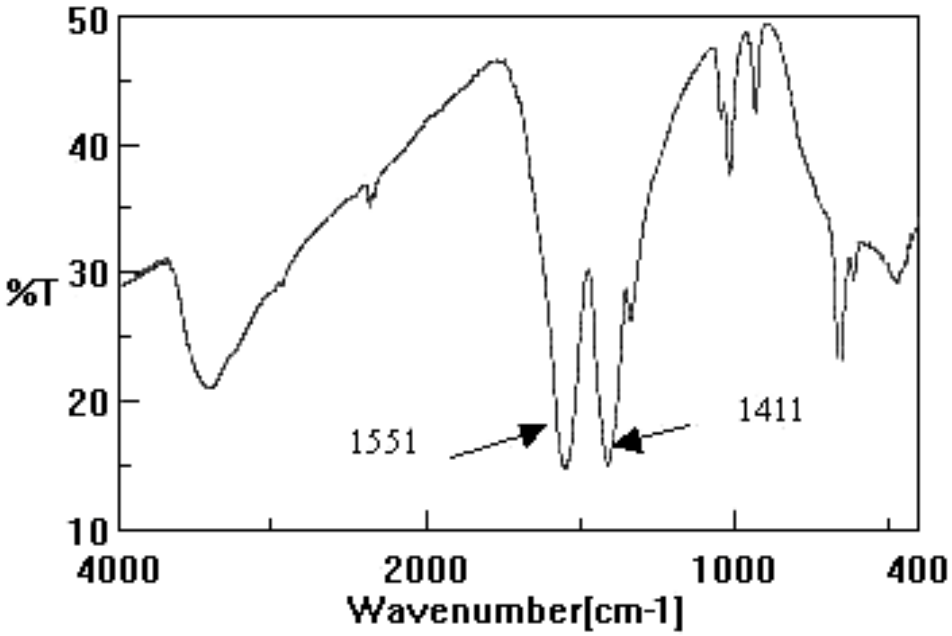

(c)

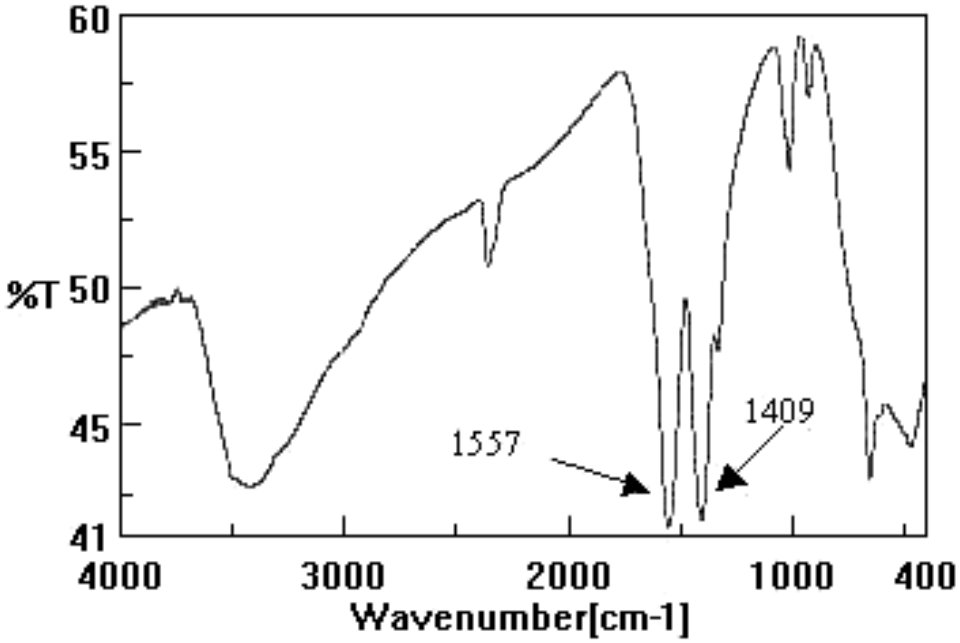
60
55
%T 50
45
41
1557
1409
4000
3000
2000
1000
400
Wavenumber[cm-1]

(a)

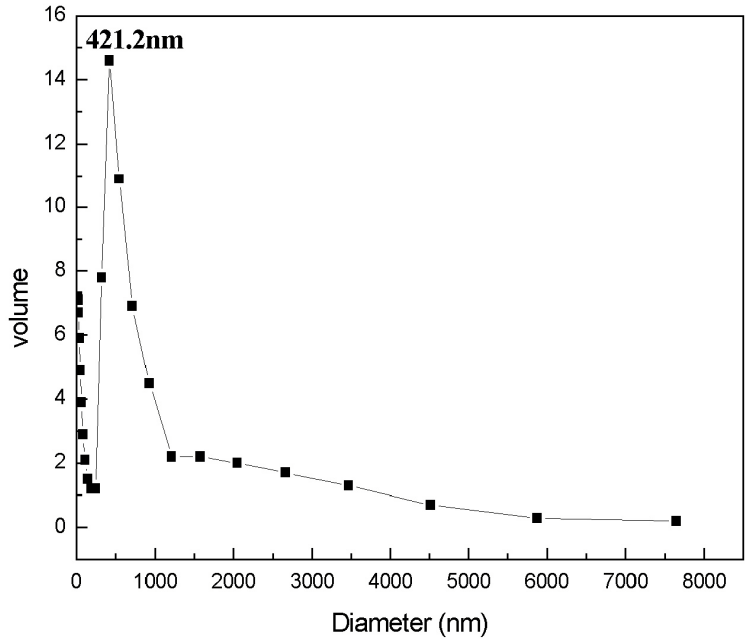

Fig. 5 The particle size distributions of (a) H.T and (b) L.T Powders

(b)

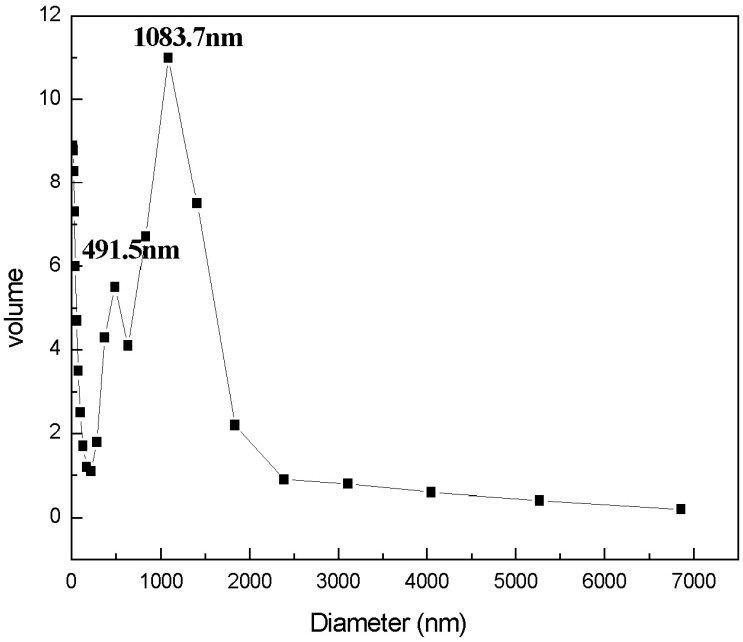
1083.7nm
491.5nm
volume
Diameter (nm)
0
2
4
6
8
10
12
0
1000
2000
3000
4000
5000
6000
7000

(a)

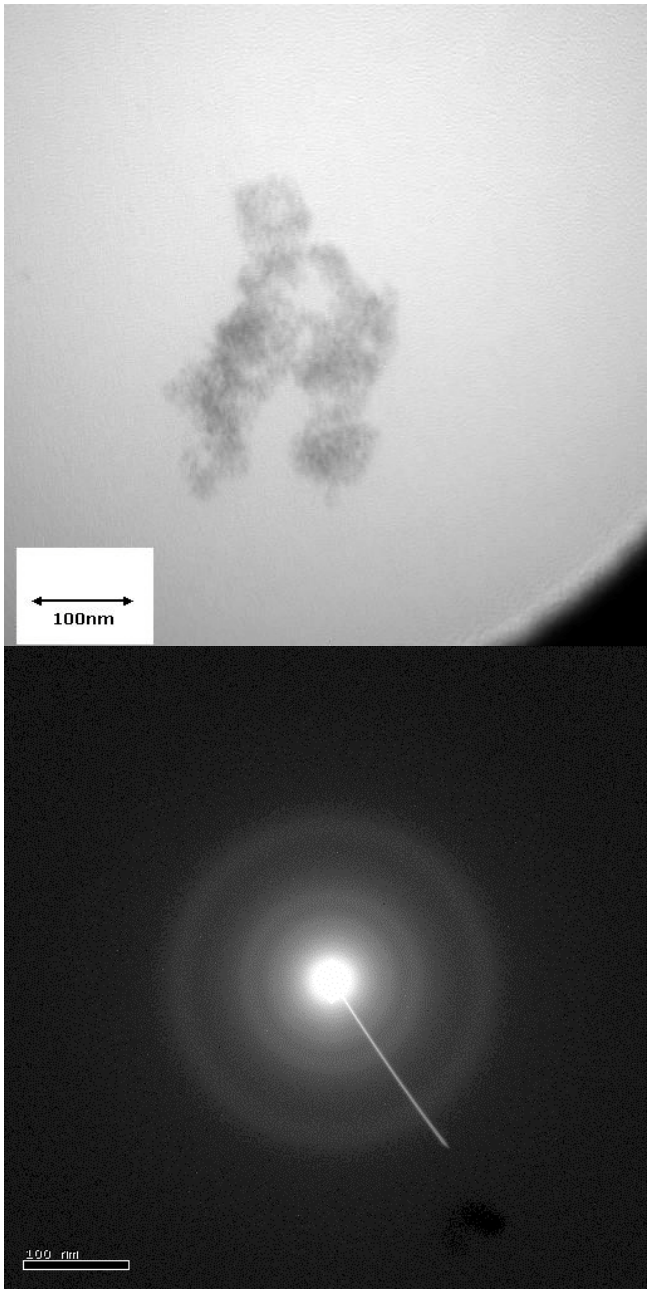

Fig.6 Bright field TEM micrographs and corresponding electron diffraction patterns for (a) H.T powders and (b) L.T powders

(b)

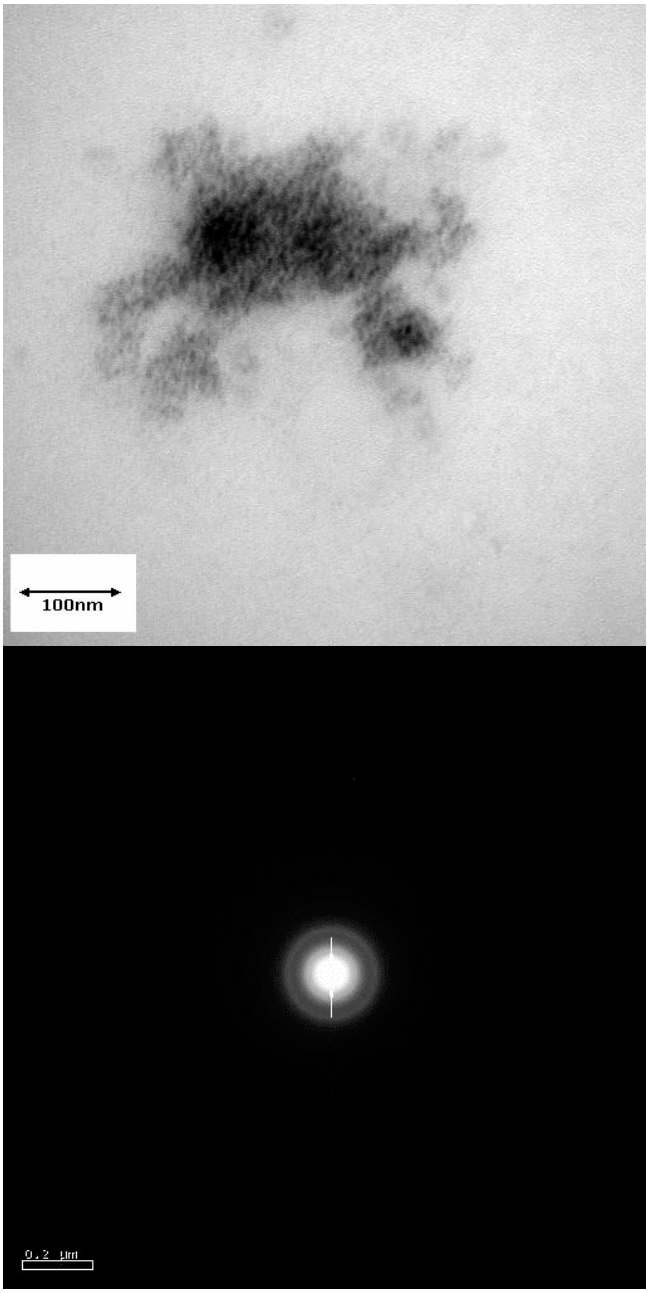
100nm
0,2 µrrl